

SESSION 5B

ESP ENERGIZATION AND CONTROL STRATEGIES

INTERMITTENT ENERGIZATION WITH HIGH FLY ASH RESISTIVITY

E. C. Landham, Jr.
Sabert Oglesby
Southern Research Institute
P.O. Box 55305
Birmingham, AL 35255

Walter Piulle
Ralph F. Altman
Electric Power Research Institute
516 Franklin Building
Chattanooga, TN 37411

George Bohn
Oklahoma Gas and Electric Company
Rt. 1, Box 83
Red Rock, OK 74651

Robert E. Kohl
Environmental Elements Corporation
P.O. Box 1318
Baltimore, MD 21203

Abstract

Modification of the energizing waveform of an electrostatic precipitator can improve performance compared to conventional energization when collecting high resistivity fly ash. Comprehensive tests of three energization methods were performed on the Sooner Station of Oklahoma Gas and Electric Company. The tests included evaluation of conventional spark-limited operation and two advanced energization methods: intermittent energization and back corona avoidance. A high resistivity Powder River Basin coal, which significantly limited performance of the precipitator, was the primary fuel burned during the test. Particle collection and power consumption indicate improved performance with both modified operating modes. Particle charge measurements and theoretical model results are used to illustrate the performance improvement mechanism.

Introduction

The negative effects on electrostatic precipitators (ESPs) of collecting the high resistivity fly ash produced by burning low-sulfur coal have been well documented. The high resistivity combined with typical values of ionic corona current results in electric fields in the precipitated dust layer sufficient to produce electrical breakdown of the flue gas. This back corona breakdown degrades ESP collection performance and increases electrical power consumption. The problem can be addressed either by reducing the resistivity of the ash or limiting the current through the dust layer. This paper is concerned with the second of those options.

Conventional ESP power supplies and controllers for ESPs apply a 60 hz, full-wave-rectified signal to the ESP electrodes. Until recently most systems provided only automatic spark-limit control, which utilizes SCR phase control to limit power input to the ESP below either the point of sparking or the output limits of the power supply. This full-power control strategy works well on low-resistivity dusts, but has little provision for avoiding back corona with high resistivity dusts. When severe back corona is present, the spark-limit type control will apply full T-R set output power to the ESP. Increasing power input to the ESP beyond the onset of back corona not only wastes power, but can actually degrade collection performance.

Modifications to conventional controls have provided several approaches to reducing the effects of back corona. Both back-corona-limit (BCL) and intermittent energization (IE) limit the average corona current through the collected dust layer to values below the onset of back corona. While BCL utilizes only the SCR phase control of conventional controls, IE uses primarily integral cycle blocking (with supplemental phase control) to accomplish the current limit. As a result, IE produces a waveform with a higher peak-to-average ratio, which has the potential to improve ESP collection performance. A major emphasis of this program was to determine if the IE waveshape provides significant advantages over conventional waveforms.

This paper describes a test program conducted to evaluate the effects of IE on an ESP collecting high resistivity fly ash. The program was conducted on Sooner Unit 2 of Oklahoma Gas and Electric Company during the summer of 1991 and evaluated three operating modes: full-power operation, IE, and BCL. Also described are the control operation, the optimization process, and the results of the comparative test program. Finally, theoretical and model analyses are used to explore the mechanisms of the performance results.

Description of Plant and Equipment

Sooner Unit 2 is a 515 MWe, Combustion Engineering, tangentially-fired boiler installed in 1980. During the test program, the unit burned a blend of fuels which included approximately 90% Western low-sulfur coal from the Powder-River-Basin (PRB) with 10% moderate-sulfur Oklahoma coal. The sulfur content of the resulting blend was less than 0.4%. The fly ash produced from the blend was dominated by the characteristics of the PRB coal with ash compositions averaging 29% calcium and 1% sodium (expressed as oxides). The ash had a high

electrical resistivity at the temperatures of the Sooner ESP, which severely limited the electrical operating conditions of the ESP.

The Sooner Unit 2 ESP was provided by the Buell Emission Control Division of Envirotech. The ESP is very large with an average specific collection area (SCA) during the program of 775 ft²/1000 acfm. The discharge electrodes are 0.105 inch diameter weighted round wires on 9 inch centers. The collecting electrodes are spaced at 9 inches and provide a total collecting area of 1,596,672 ft² grouped into seven fields. The ESP is powered by 12 transformer-rectifier (T-R) sets per field, for a total of 84 T-R sets.

The ESP T-R set controls were retrofitted to the Sooner ESP prior to the test program by Environmental Elements Corporation. The controls originally had the capability for full-power, spark-limit operation or energy management. The capability for IE and BCL were added to the controls for the test program.

Control Strategy and Optimization

For IE to provide maximum benefit to the operation of the ESP, the applied waveform must be optimized for the operating conditions. The goal of IE optimization was to maximize the peak values of the ESP voltage and current waveforms while maintaining an average current through the dust layer just below back corona onset. The only concern during optimization was maximizing ESP collection efficiency, and no consideration was given to optimizing power savings. Although reduced power consumption is a definite benefit of IE operation, the power savings incurred during the test program were incidental.

Critical to the optimization process is accurate detection of back corona. When back corona is present in the dust layer, the regenerative feedback effect of the positive ion discharge reduces effective interelectrode resistance and increases ionic current dramatically. The increased current causes the ESP capacitance to discharge more rapidly than when back corona is not present. The more rapid discharge results in reduced voltage values on the RC decay portion of the ESP voltage waveform, as illustrated in Figure 1. Because of the hysteresis associated with back corona discharge, reduced voltage values also are seen in the waveform minimum.

During the Sooner test program, the onset of back corona was detected by observing the minimum value of the voltage waveform. Figure 2 shows the minimum waveform value during IE as a function of the number of half-cycles deenergized for one field of the Sooner ESP. These data indicate that the minimum waveform value was maximized at 6-8 half-cycles off and that the value decreased with both longer and shorter off-times. The decrease with shorter off-time is caused by back corona, while the decrease with longer off-time is caused by increased time for the ESP capacitance to discharge. Manual adjustments around the point of the highest waveform minimum indicated that the addition of 2 extra half-cycles to the deenergized time produced the greatest reductions in stack opacity. The highest waveform minimum plus two half-cycles deenergized was used as the optimized operating point during the test program.

To provide maximum performance, all 84 of the Sooner ESP T-R sets had to be optimized for the current operating conditions. Because of changes in gas temperature during the day and resulting changes in ash resistivity, the optimized operating point varied with time. Manually optimizing the controls throughout the day would have been a massive undertaking and probably would not have produced truly optimized performance. Therefore, the Environmental Elements controls were programmed to automatically seek the optimized operating point every 15 minutes. The automatic optimization process for IE began with waveform off-times much longer than necessary to eliminate back corona and gradually reduced the off-time until the waveform minimum value decreased, indicating back corona onset. After quenching the back corona, operation proceeded at the newly determined optimization point.

The BCL mode of operation also seeks the maximum current through the dust layer without causing back corona, but achieves the current control through a more conventional method. While gradually increasing T-R current output, the control system detected the point where increasing current resulted in a drop in the minimum value of the ESP voltage waveform. T-R power output was then reduced slightly to operate just below the back corona point. Extensive manual measurements of ESP voltage-current characteristics and monitoring the automatically selected operating point confirmed that the controls were producing optimized operation at the knee of the V-I curve. The BCL optimization also occurred every 15 minutes during the test program.

When IE is applied to an ESP collecting low resistivity dust, the ionic current through the dust layer will be significantly reduced compared to normal, full-power operation. The reduced dust layer current with IE will reduce the electrical force holding the dust on the collecting electrode, which can result in increased rapping emissions, if the same rapping forces are applied. This effect has been observed in the field, and has been generally treated by reducing rapping intensity. At Sooner, however, excessive rapping puffs were not experienced, probably because of the already low useful (or non-back corona) current densities related to the high resistivity. No adjustments were made to the rapping strategy for IE operation.

Test Results

Ash Resistivity and ESP Electrical Conditions

The electrical resistivity of the fly ash entering the Sooner Unit 2 ESP was measured in situ with a point-plane probe during each day of the test program. The average resistivity values for each of the three test phases are shown in Table 1. Very consistent results were obtained which do not indicate any significant bias in the performance results because of changes in ash properties. The resistivity values were all around 3×10^{11} ohm-cm, a value which is considered moderately high, and is in general agreement with in-situ values observed with other PRB coal ashes. Consistent with the low coal sulfur, high ash calcium, and high measured resistivity, no vapor-phase SO_3 could be detected at the inlet to the ESP.

The electrical conditions inside the ESP resulting from the ash resistivity are indicated by the voltage-current (V-I) curves, which are plotted as voltage vs dust layer current density, in Figure 3. The ESP fields included in the figure are spaced approximately equally down the length of the ESP from inlet to outlet. The V-I curves indicate that the electrical conditions in most of the ESP fields were very poor with severe back corona in all but the inlet field (2G12). The inlet field was limited to low current density by sparking. The onset of back corona occurred below 10 nA/cm^2 for most fields, with breakdown as low as 3 nA/cm^2 in some fields. Breakdown at these current densities is usually related to a higher resistivity than that indicated by the in-situ data. Comparison to a database which relates resistivity to typical ESP electrical conditions [1] suggests that the Sooner V-I data are more reasonable for resistivity values in the 10^{12} ohm-cm range. This disagreement has been observed with other PRB coals and might be a result of sodium depletion or unusually thick dust layers. Regardless of the cause, the severe back corona present in the Sooner ESP makes it a prime candidate for the application of either IE or BCL.

The average electrical conditions of the ESP during the comprehensive tests are shown in Table 2. Comparison of the current density values from each of the test programs indicates that both IE and BCL modes produced similar limits on dust layer current. The average current density in both modes was below 6 nA/cm^2 , with the outlet fields limited to below 10 nA/cm^2 . These values are consistent with elimination of the back corona observed in the Sooner V-I curves. The low values with IE and BCL are in contrast to the full-power case, which had an average of 29 nA/cm^2 and over 50 nA/cm^2 in the outlet field. The extra current input during full-power operation was wasted.

The last column in Table 2 contains the average number of deenergized half-cycles for each field during IE operation. Although in actual practice the number of deenergized half-cycles must be an integer multiple of 2, the numbers shown in the table are averages of 12 T-R sets, each of which may have a different operating point. The average number of deenergized half-cycles for the IE test was slightly over 8, for an IE ratio of 1/9. The inlet field was not included in the IE test because of its already low current density from sparking. The highest off-times were observed in the middle of the ESP rather than in the outlet fields as theory would predict. This is in agreement with the V-I curves which show poorer electrical conditions in that area also. The reason for the poorer electrical conditions in the middle of the ESP is unknown, but could be related to ash deposit characteristics, electrode alignment, or gas temperature gradients.

The main difference between IE and BCL operation is indicated by the voltage data in Table 2. IE produced by far the highest peak voltage values and the lowest average voltage values of any test condition. The peak-to-average voltage ratio for the fields operating in IE ranged from 2.11 to 3.03 with most peak values over 50 kV. The BCL case produced a peak-to-average range of 1.09 to 1.23 with all peak values at or below 36 kV. However, the BCL mode provided average voltage values 28% higher than the IE case. The changes in peak and average voltages have competing effects which are discussed in a later section.

ESP Performance and Power Consumption

The measured performance of the ESP for the three operating modes is shown in Table 3. These data indicate that IE operation provided the best particle collection performance, with BCL mode second, and full-power operation producing the poorest collection. Because of the large SCA of the Sooner ESP, the particle emission rates were below the compliance limit of $0.03 \text{ lb}/10^6 \text{ Btu}$ despite the comparatively poor performance during full-power operation. Compared to full-power, BCL operation reduced the particle emissions to 62% of full-power, while IE dropped emissions to 36% of the full-power case. Opacity reductions were significant and in the same direction, but were by smaller percentages than the mass emissions.

The electrical power consumption of the ESP T-R sets during each of the three tests is also shown in Table 3. These data indicate that IE and BCL reduced power consumption to 27% and 19%, respectively, of full-power case. Thus, BCL did result in a somewhat larger power savings than did IE, but at the cost of slightly decreased collection performance.

The particle size dependent collection efficiency of the ESP is shown for IE and BCL modes in Figure 4. No comparable data were obtained for the full-power condition in order to limit the time spent at that relatively poor performance level. These data indicate that IE improved performance for all particle sizes down to the lower limit of the measurement at $0.5 \mu\text{m}$. The data do indicate that a larger increase in collection efficiency occurred for large particles than for those around $1 \mu\text{m}$. Since particles around $1 \mu\text{m}$ affect opacity more than do large particles, per unit mass, this accounts for the relative differences observed for particle emissions and opacity.

ESP Modeling and Performance Analysis

Under the reduced power conditions necessary to avoid back corona with high resistivity dust, the waveshape of IE has some potential theoretical advantages over conventional waveshapes, although there are competing effects. Because of the relatively slow movement of the particles through the ESP compared to the cycle time of the energizing waveform, the saturation charge on the fly ash particles should be a function of the peak electric field in the ESP. However, the low mobility of the charged particles makes particle collection approximately a function of the average electric field in the region close to the collecting plate. Thus, the higher peak voltage values with IE should result in increased levels of field-induced charge on particles, while the reduced average voltage will cause lower values of collecting field at the plate. Since the current densities are the same for IE and BCL, diffusion charging should not be affected.

The EPA/SRI Mathematical Model of ESP Performance [2] was used to simulate and analyze the performance of the Sooner ESP. However, to accurately simulate the conditions of IE, changes had to be made to the model. The model uses the peak-to-average voltage ratio and the average voltage to determine the peak interelectrode electric fields for calculation of particle charge values resulting from field and field-enhanced-diffusion charging. However, in the previous model version, the peak-to-average ratio was a single entry for the entire ESP, which the data from

Table 2 show is not appropriate for IE. The model was modified to allow individual entries of peak-to-average ratio for each field. It was also determined that the peak field value was not correctly used in the calculation of field-enhanced diffusion charging. This oversight was corrected and the result evaluated for conventional ESPs in the EPRI database [1]. For conventional (Non-IE) operation the changes produced only minor effects on the model calculations.

Figure 5 compares the model predictions of particle penetration for the Sooner ESP to the measured values for each of the three operating modes. Since BCL is the simplest case to model (conventional waveform and no back corona), the non-ideal conditions of the model were adjusted to obtain agreement for this case. Values of sneakage and gas flow uniformity of 0.26 and 0.15, respectively, gave the best agreement. Although this value of sneakage is somewhat higher than some would expect [1], according to our experience this is typical for very large ESPs with SCAs over 500 ft²/1000 acfm. That is, very large ESPs do not seem to work as well as the model would suggest, probably because of the relative contributions to total emissions of non-ideal effects for small and large ESPs.

Using the non-ideal conditions which gave agreement with BCL, the model results using IE conditions gave almost perfect agreement with the measured IE penetration. The model also correctly predicted that the particle emissions would be reduced by more than the opacity. The reason for the improved performance with IE is illustrated by Figures 6 and 7. The curves on Figure 6 show the charge on individual particles as a function of particle size computed by the ESP model for IE (solid) and BCL (dashed). On average, the model computed 40% higher particle charge because of the higher IE peak voltages, with increasing effect for larger particles. The charge on particles smaller than 0.2 μm , which are totally dependent on diffusion charging, should be the same for both modes because of the similar current densities. The computed charge levels are in excellent agreement with the particle charge values measured at the outlet of the ESP with a Millikan oil-drop apparatus (symbols on Figure 6). Figure 7 compares the model calculated IE and BCL electric field profiles from the wire to plate for the outlet field of the ESP. The field at the plate is calculated to be 20% lower as a result of the reduced average voltage with IE. Since collection is a function of the product of particle charge and collecting electric field, one would expect these relative variations to result in the net performance increase observed with IE.

The results of the model calculations for full-power operation are also shown on Figure 5. However, this case is useful only to illustrate how inappropriate it is to use measured electrical conditions to predict performance when back corona is present. As expected, the model predicted penetrations which were over an order of magnitude too low for the full-power case, indicating that most of the back corona power was not useful for charging and collecting particles. Indeed, the poorer performance with full-power than with either of the other modes indicates that the back corona power input was not just wasted, but significantly degraded performance.

Summary and Conclusions

A comprehensive test program was conducted on the effects of intermittent energization and back-corona-limit on the performance of an ESP collecting high resistivity fly ash. Most fields of the ESP were operating in severe back corona during full-power operation. The following observations can be made concerning the results of the study.

Eliminating the back corona power by reducing dust layer current without changing the shape of the voltage waveform improved ESP collection performance and reduced power consumption. Operation with the back-corona-limit mode dropped particle emissions to 62% of the full-power level and reduced power consumption to 19% of full-power.

Using intermittent energization to reduce dust layer current while increasing peak voltage values resulted in substantially better performance than was obtained with the conventional waveform. IE reduced particle emissions by almost a factor of 2 compared to BCL, and by almost a factor of 3 compared to full-power. IE reduced power consumption to 27% of the full-power value, but did require 44% more electrical power than BCL mode.

The improved collection with BCL is attributed to elimination of the back corona in the ESP. The further improvement obtained with IE was caused by increased peak electric field which resulted in increased charge for all particle sizes larger than about 0.2 μm . The increased particle charge more than compensated for the decreased electric field at the plate produced by the lower average voltages with IE.

The primary emphasis during optimization of the IE waveform during the program was to have the shortest deenergized time interval with reasonably high peak values. However, little effort was put into actually optimizing the peak-to-average voltage ratio for a particular current density, either through control strategy or hardware modifications. Given the apparent mechanisms controlling IE performance, additional effort to increase peak voltages could provide further performance improvements.

The higher power consumption values for IE than for BCL, despite apparently lower average values of T-R secondary power, appear to indicate higher power losses during IE operation. Equipment optimization for the IE waveshape might provide additional reductions in power consumption.

With appropriate modifications and measured electrical conditions, the EPA/SRI ESP model did appear to accurately predict ESP performance with IE. The computed values of particle charge agreed with field measurements. However, a proven correlation does not yet exist which relates IE electrical conditions to resistivity, electrode geometry, and T-R specifications. Such a correlation must be developed to provide a general understanding of IE performance effects and to allow accurate predictions of IE performance effects for ESPs for which actual IE operating conditions are not available.

References

1. J. L. DuBard and R. S. Dahlin. Precipitator Performance Estimation Procedure. Electric Power Research Institute. Palo Alto, California. EPRI CS-5040. February 1987.
2. M. G. Faulkner and J. L. DuBard. A Mathematical Model of Electrostatic Precipitation (Revision 3): Vol. I. U. S. Environmental Protection Agency. Research Triangle Park, North Carolina. EPA-600/7-84-069. July 1984.

Operating Mode	Gas Temperature, °F	Dust Resistivity, ohm-cm
Intermittent Energization	302	3.62×10^{11}
Back-Corona-Limit	313	3.43×10^{11}
Full-Power	310	2.80×10^{11}

Table 2
Sooner ESP Electrical Operating Conditions

ESP Field	Voltage, kV			Peak/Avg Voltage Ratio	Current Density, nA/cm ²	Average Off Half-Cycles
	Peak	Average	Minimum			
Intermittent Energization						
1	42.6	39.8	38.3	1.07	2.87	0.0
2	55.2	26.2	21.3	2.11	4.96	9.0
3	51.1	21.9	17.2	2.33	4.78	9.7
4	48.3	17.9	13.1	2.70	4.81	10.5
5	52.2	17.4	12.0	3.00	6.32	10.9
6	52.1	17.2	11.7	3.03	7.19	9.2
7	51.9	17.5	11.8	2.97	8.75	8.3
Average	50.5	22.6	17.9	2.46	5.67	8.2
Back-Corona-Limit						
1	42.7	40.0	38.3	1.07	2.59	
2	36.0	33.0	30.3	1.09	3.12	
3	30.3	27.3	26.0	1.11	3.36	
4	29.3	25.0	22.7	1.17	4.16	
5	30.0	25.3	22.0	1.19	6.52	
6	32.0	26.3	22.3	1.22	8.32	
7	32.3	26.3	21.7	1.23	9.82	
Average	33.2	29.0	26.2	1.15	5.41	
Full-Power						
1	42.5	39.8	38.1	1.07	2.59	
2	45.6	35.3	27.8	1.29	16.81	
3	39.2	30.0	23.3	1.31	21.31	
4	37.7	28.8	20.2	1.31	30.95	
5	39.1	28.0	19.0	1.40	38.35	
6	39.2	28.1	20.1	1.40	37.84	
7	42.9	31.5	19.4	1.36	53.17	
Average	40.9	31.6	24.0	1.30	28.72	

Table 3 Sooner ESP Performance Summary					
Operating Mode	ESP Efficiency, %	Particle Penetration, %	Particle Emissions, lb/10 ⁶ Btu	Stack Opacity, %	Power Consumed, kW
IE	99.77	0.23	0.0067	10.8	404
BCL	99.65	0.35	0.0115	13.2	281
Full-Power	99.48	0.52	0.0185	16.2	1497

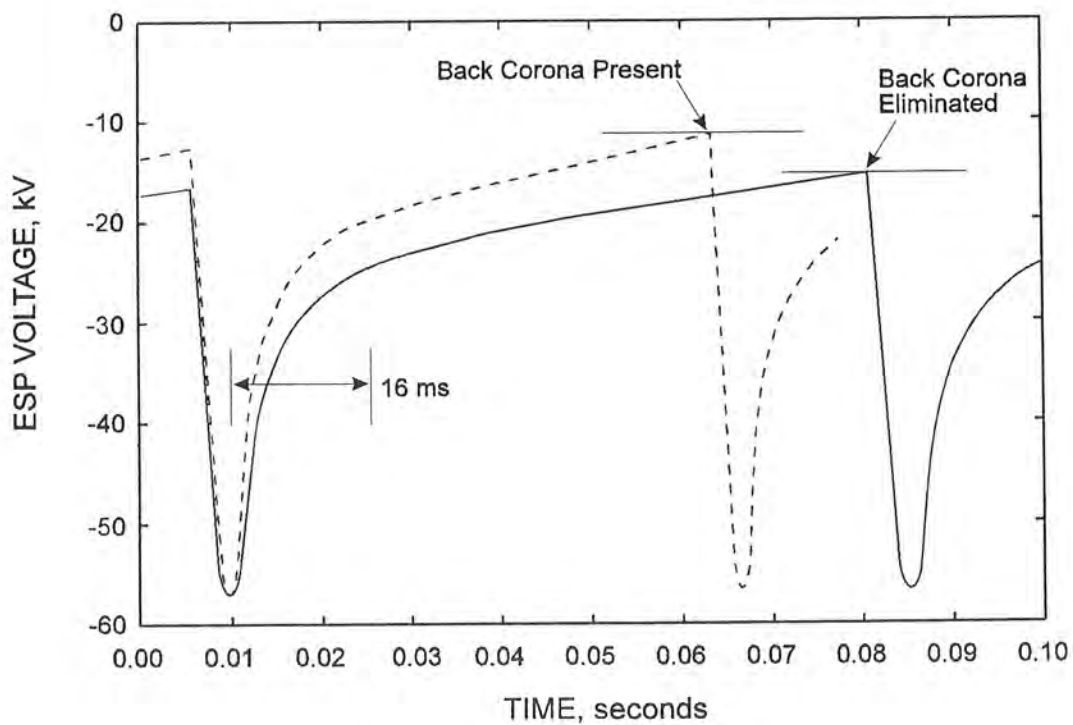


Figure 1. Effect of Back Corona on ESP Waveform

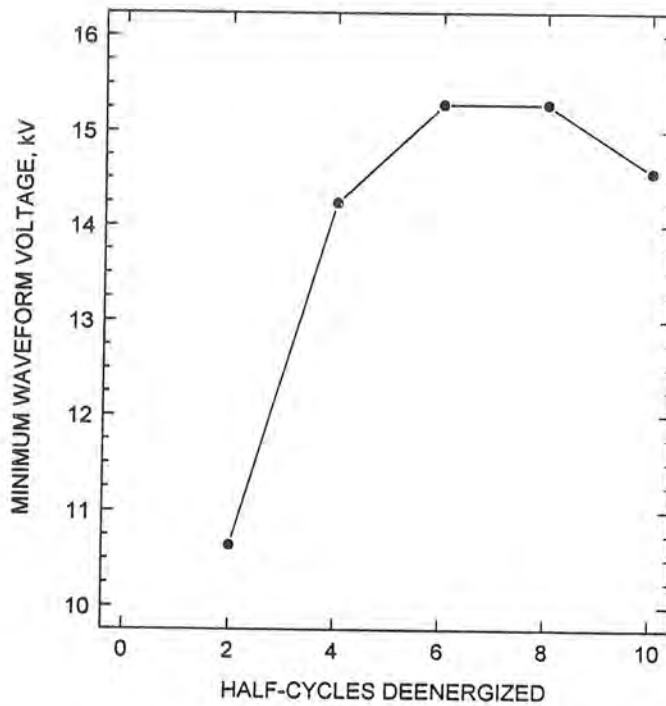


Figure 2. Minimum IE Waveform Voltage as a Function of Half-Cycles Deenergized.

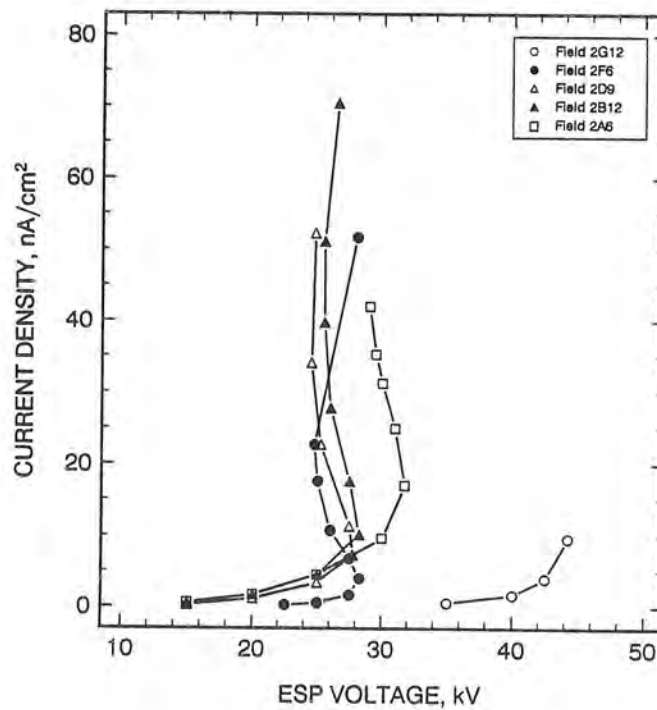


Figure 3. ESP Electrical Characteristics during Full-Power Operation.

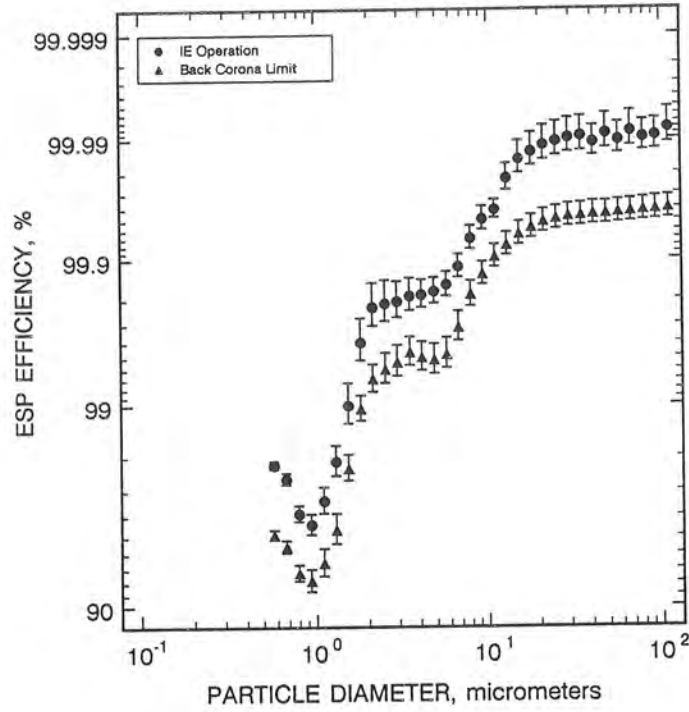


Figure 4. ESP Collection Efficiency as a Function of Particle Size for IE and BCL Operation.

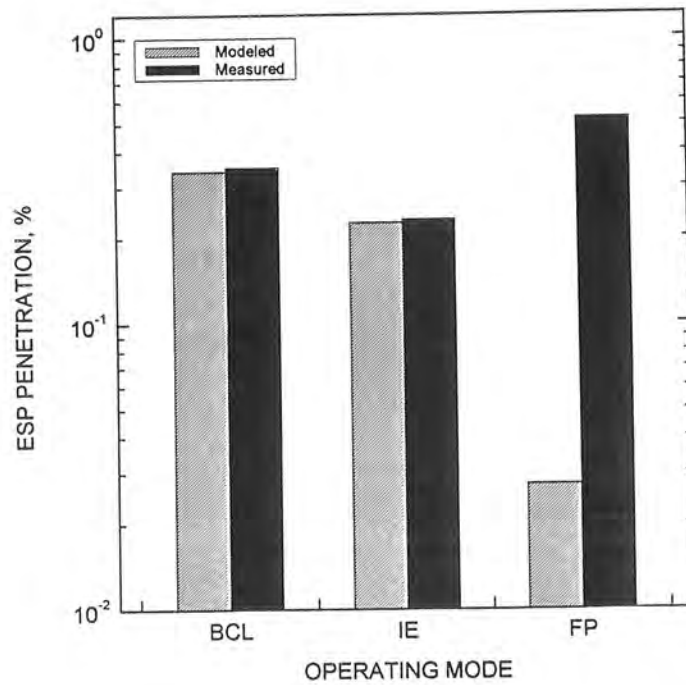


Figure 5. Comparison of Measured and Model Computed ESP Performance.

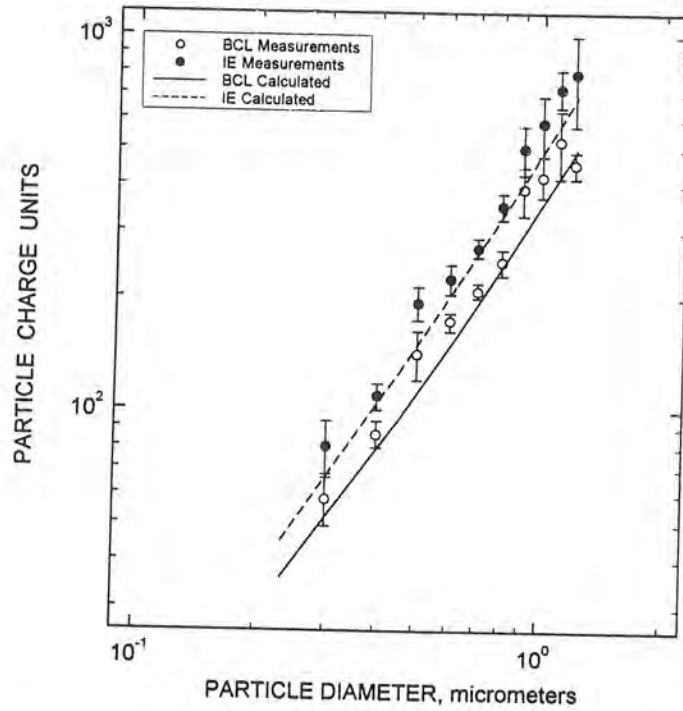


Figure 6. Comparison of Measured and Model Computed Particle Charge Values.

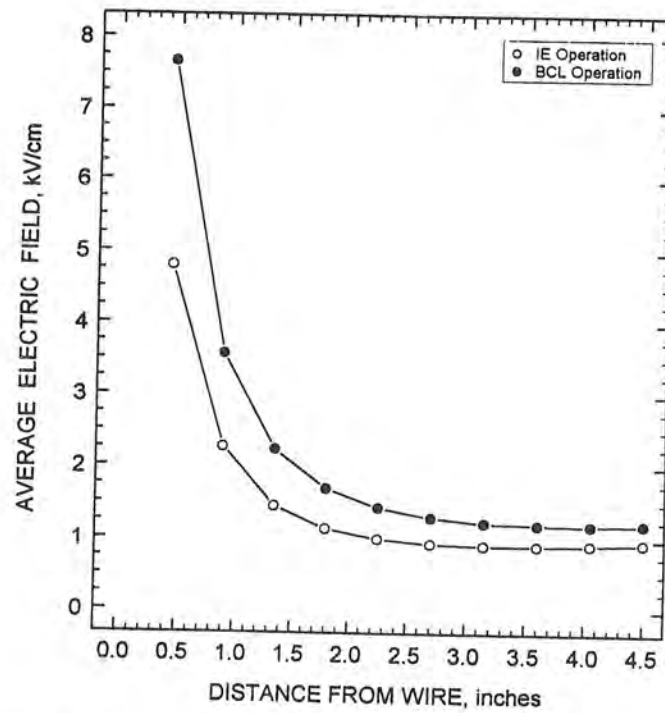


Figure 7. Model Computed Electric Field Profiles for IE and BCL Operation.